https://doi.org/10.5194/acp-2019-685
Preprint. Discussion started: 2 September 2019

Atmospheric Chemistry and Physics Discussions

Regional variability in black carbon and carbon monoxide ratio from long-term observations over East Asia: Assessment of representativeness for BC and CO emission inventories

Yongjoo Choi[1*], Yugo Kanaya[1], Seung-Myung Park[2], Atsushi Matsuki[3], Yasuhiro Sadanaga[4], Sang-Woo Kim[5], Itsushi Uno[6], Xiaole Pan[7], Meehye Lee[8], Hyunjae Kim[2], Dong Hee Jung[2]

[1] Research Institute for Global Change, Japan Agency for Marine-Earth Science and Technology (JAMSTEC), Yokohama, 2360001, Japan

[2] Division of Climate & Air Quality Research, National Institute of Environmental Research, Kyungseo-dong, Seo-Gu, Incheon 404170, Korea

[3] Institute of Nature and Environmental Technology, Kanazawa University, Kanazawa 9201192, Japan

[4] Department of Applied Chemistry, Graduate School of Engineering, Osaka Prefecture University, 1-1 Gakuen-cho, Naka-ku, Sakai, Osaka 5998531, Japan

[5] School of Earth and Environmental Sciences, Seoul National University, Seoul, Korea

[6] Research Institute for Applied Mechanics, Kyushu University, Kasuga Park 6-1, Fukuoka, 816-8580, Japan

[7] Institute of Atmospheric Physics, Chinese Academy of Sciences, Beijing, China

[8] Department of Earth and Environmental Sciences, Korea University, Seoul, Korea

*Correspondence to: Yongjoo Choi (choingjoo@jamstec.go.jp)

Prepared for *Atmospheric Chemistry and Physics*

Submitted in July 2019

https://doi.org/10.5194/acp-2019-685
Preprint. Discussion started: 2 September 2019

Atmospheric Chemistry and Physics Discussions

Abstract

The BC/CO emission ratios were estimated and compiled from long-term, harmonized observations of the ΔBC/ΔCO ratios under conditions unaffected by wet deposition at four sites in East Asia, including two sites in Korea (Baengnyeong and Gosan) and two sites in Japan (Noto and Fukuoka). Extended spatio-temporal coverage enabled estimation of full seasonality and elucidation of the emission ratio in North Korea, for the first time. The estimated ratios were used to validate the Regional Emission inventory in Asia (REAS) version 2.1 based on six study domains (East China, North China, Northeast China, South Korea, North Korea, and Japan). We found that the ΔBC/ΔCO ratios from four sites converged into a narrow range (6.2 – 7.9 ng m^{-3} ppb^{-1}), suggesting consistency in the results from independent observations and similarity in source profiles over the regions. The BC/CO ratios from the REAS emission inventory (7.7 ng m^{-3} ppb^{-1} for East China – 23.2 ng m^{-3} ppb^{-1} for South Korea) were overestimated by factors of 1.1 for East China to 3.0 for South Korea, whereas the ratio for North Korea (3.7 ng m^{-3} ppb^{-1} from REAS) was underestimated by a factor of 2.0, most likely due to inaccurate emissions from the road transportation sector. Seasonal variation in the BC/CO ratio from REAS was found to be the highest in winter (China and North Korea) or summer (South Korea and Japan), whereas the measured ΔBC/ΔCO ratio was highest in spring in all source regions, indicating the need for further characterization of seasonality when creating a bottom-up emission inventory. At levels of administrative districts, overestimation in Seoul, the southwest regions of South Korea, and Northeast China was noticeable, and underestimation was mainly observed in the western regions in North Korea, including Pyongyang. These diagnoses are useful for identifying the regions where revisions in the inventory are necessary, providing guidance for refinement of BC and CO emission rate estimates over East Asia.

https://doi.org/10.5194/acp-2019-685
Preprint. Discussion started: 2 September 2019

Atmospheric Chemistry and Physics Discussions

1 Introduction

Black carbon (BC), emitted from incomplete combustion of fossil fuel and/or biomass burning, absorbs solar radiation and reduces the surface albedo of snow/ice after dry/wet deposition (Samset, 2018; Bond et al., 2013); thereby augmenting the global warming trend primarily induced by increased levels of carbon dioxide (CO_2) (Ramanathan and Carmichael, 2008; Jacobson, 2001; Myhre et al., 2013). In addition to global warming effects, BC is significantly associated with cardiovascular mortality (Smith et al., 2009; Geng et al., 2013), and is more related to health effects than $PM_{2.5}$ (particulate matter having an aerodynamic diameter $\leq$ 2.5 μm) (Janssen et al., 2011, 2012; Loomis et al., 2013).

In particular, the BC emission from China, which accounted for 31% of the total annual global emission in 2012 (Crippa et al., 2018), showed an increasing trend from 1970 to 2012 (Kurokawa et al., 2013; Ohara et al., 2007; Crippa et al., 2018). To enhance the understanding of the behavior of BC in the atmosphere, it is essential to obtain a reliable BC concentration along with model simulation based on accurate bottom-up emission inventories. The bottom-up emission inventories may be subject to large uncertainties associated with emission factors from various types of combustion sources, countries and species (Kurokawa et al., 2013), although the uncertainty in BC emission decreased from 160.2% in 1970 to 74.3% in 2012 (Crippa et al., 2018). BC and carbon monoxide (CO) are byproducts of incomplete combustion of carbon-based fuels, and the ratio between ΔBC (difference from the baseline level) and ΔCO could be a useful parameter for characterizing combustion types. Using those characteristics, past studies dealt with the ΔBC/ΔCO ratio to identify the emission source types (Guo et al., 2017; Pan et al., 2011; 2013; Zhu et al., 2019) and/or validate BC emissions from bottom-up inventories (Han et al., 2009; Wang et al., 2011; Verma et al., 2011; Sahu et al., 2009; Kondo et al., 2006). However, it was hard to diagnose the accuracy of emission inventories over East Asia from those studies because either data from short, intensive measurement periods at a single site were used or the studied source regions did not necessarily match the administrative districts for which a detailed emission inventory was constructed. In addition, BC concentrations could differ depending on the instruments and operation protocols used for observations—such discordance yet poses a major obstacle to obtaining a comprehensive understanding. Kondo (2015) compiled ΔBC/ΔCO ratios from systematic observations in Asia. However, information during the 2010s, when emission patterns changed significantly, has not

https://doi.org/10.5194/acp-2019-685
Preprint. Discussion started: 2 September 2019

Atmospheric Chemistry and Physics Discussions

been covered. Kanaya et al. (2016) used observations at Fukue Island for 6 years (2009-2015) to derive a region-specific ΔBC/ΔCO emission ratio. However, the season was limited to autumn-spring, and the footprint over each source region was still limited, as observations at a single site were analyzed.

In this study, we investigated the ΔBC/ΔCO ratio from long-term measurements at four measurement sites (two Korean and two Japanese sites which measured for more than a year) over East Asia in order to comprehensively evaluate the Regional Emission inventory in Asia (REAS) emission inventory (Kurokawa et al., 2013) for BC and CO with sufficient spatio-temporal coverage. Improved spatio-temporal coverage enabled estimation of full seasonality and elucidation of the emission ratio from North Korea, for the first time. By comparing the regional and seasonal ΔBC/ΔCO ratio between the REAS emission inventory and the measurements, this study identifies the points of improvement in the bottom-up emission inventories.

2 Methodology

2.1 Measurement sites and periods

Figure 1 shows the location of measurement sites in this study. Both Baengnyeong (124.63 °E, 37.97 °N) and Gosan (126.17°E, 33.28 °N) are representative background sites in Korea. The Baengnyeong site is an intensive measurement station operated by the Korean Ministry of Environment. The Gosan site was a supersite of many international campaigns, such as Aerosol Characterization Experiments (ACE)-Asia (Huebert et al., 2003), Atmospheric Brown Cloud (ABC) (Nakajima et al., 2007) and Cheju ABC Plume–Monsoon Experiment (CAPMEX) (Ramana et al., 2010). Since the two sites in Korea are located in the western region of the Korean peninsula with similar longitudes but different latitudes, those sites are suitable for monitoring pollutant transport from China, North Korea (especially Baengnyeong) and South Korea. In Japan, the Fukuoka site (33.52 °N, 130.47 °E) is located at the Chikushi Campus of Kyushu University located in the suburbs of Fukuoka, and the site is the largest center of commerce on the island of Kyushu (Itahashi et al., 2017; Uno et al., 2017). The Noto site (37.45 °N, 137.36 °E) is located at the Ground-based Research Observatory (NOTOGRO), which has been apart from Kanazawa and Toyama, the nearest provincial cities, by

https://doi.org/10.5194/acp-2019-685
Preprint. Discussion started: 2 September 2019

Atmospheric Chemistry and Physics Discussions

113 approximately 115 km southwest and 85 km south, respectively. Therefore, Noto is a suitable
114 place for monitoring the background concentration and/or outflows of pollution from the Asian
115 continent (Ueda et al., 2016). The measurement periods were commonly in the early 2010s,
116 while slight difference was present among the sites (Table 1). The longest measurement period
117 was in Noto for approximately six years (from 2011 to 2016), followed by Baengnyeong (five
118 years), Gosan (three years), and Fukuoka (one and a half years). The measurement in
119 Baengnyeong did not include 2011 to 2012 due to the absence of CO data.

120

121 **2.2 Instruments**

122 It is crucial to ensure reliable atmospheric BC concentrations, which were measured by
123 different instruments, by excluding the effects of co-existing scattering particles. To keep the
124 harmonization, we consider BC concentrations to be reliable when the data were measured by
125 pre-validated instruments reported to have good agreement between instruments, including
126 OC-EC analyzers (Sunset Laboratory Inc., USA) with optical corrections, continuous soot-
127 monitoring systems (COSMOS) and multi-angle absorption photometer (MAAP 5012 Thermo
128 Scientific) (Kanaya et al., 2008, 2013).

129 Hourly elemental carbon (EC) concentrations in $PM_{2.5}$ at the Baengnyeong site were
130 measured by a model-4 semi-continuous OC-EC field analyzer using the thermal/optical
131 transmittance (TOT) method and the non-dispersive infrared (NDIR) method based on NIOSH
132 method 5040 (NIOSH, 1996). The particles passed through a $PM_{2.5}$ cyclone with 8.0 L/min and
133 a carbon impregnated multi-channel parallel plate diffusion denuder (Turpin et al., 2000), and
134 were collected on a quartz fiber filter during 45 min. OC and EC were then analyzed during
135 the last 15 min. The detection limit of EC, which is defined as twice the average of the field
136 blanks, was reported to be 30 ng m^{-3}, and the precision of EC was 7.5% (Park et al., 2013).

137 At both Noto and Fukuoka sites, $PM_{2.5}$ BC concentrations were measured by using a MAAP.
138 The BC concentration is converted from the absorption coefficients, which were determined
139 by measuring both the transmittance and reflectance of a filter loaded with aerosols. Because
140 the MAAP installed a light detector that locates light reflected from the filter at 130° and 165°
141 from the illumination direction (Petzold et al., 2005), the MAAP can correct for scattering
142 particle effects. It should be noted that we used a different mass absorption efficiency (MAE)

https://doi.org/10.5194/acp-2019-685
Preprint. Discussion started: 2 September 2019

Atmospheric Chemistry and Physics Discussions

value of 10.3 m^2 g^{-1}, as suggested by Kanaya et al. (2013), instead of the default MAE of 6.6 m^2 g^{-1}, which showed perfect correlation with the COSMOS BC concentration (Kanaya et al., 2013). The reported minimum detection limit of MAAP was different depending on the averaging time as 12 ng m^{-3} for one hour and 64 ng m^{-3} for one minute by applying the revised MAE (10.3 m^2 g^{-1}).

The Gosan site has monitored BC concentration using a continuous light absorption photometer (CLAP) with three wavelengths including 467, 528, and 652 nm (Cho et al., 2019). Through PM_1 and PM_{10} impactors, which switched every 30 min, the particles were collected on the 47-mm diameter glass-fiber filters (Pallflex type E70-2075W). The volumetric flow rate was 1 L/min. The raw absorption coefficient of the CLAP was corrected using the Bond et al. (1999) methods to eliminate effects due to filter loading error. The absorption coefficient at 528 nm was used for converting the BC concentration by applying 10 m^2 g^{-1} for MAE. In this study, we used the PM_1 BC concentration because the BC particles mainly exist in less than 1 μm (Miyakawa et al., 2017; Bond et al., 2013). Although the uncertainty derived from scattering particles was reported to be ~25% at Gosan (Ogren et al., 2017), the BC from CLAP was verified by comparison with a co-located semi-continuous OC-EC field analyzer (Lim et al., 2012). The slope of the best fit line through the origin was close to one as 1.17, implying that the PM_1 BC concentration from CLAP was consistent well with that from $PM_{2.5}$ EC.

Hourly CO concentrations were measured by gas filter correlation CO analyzer (Model 300EU, Teledyne-API Inc.) for Baengnyeong and nondispersive infrared absorption photometer (48C, Thermo Scientific) for the other three sites.

2.3 ΔBC/ΔCO ratio and allocation of the dominant emission region

To identify the origin of BC and CO emission sources, backward trajectories at 500m during the past five days (120 hours) were calculated by the Hybrid Single Particle Lagrangian Integrated Trajectory (HYSPLIT) 4 model (Draxler et al., 2018) for every six hour intervals (00, 06, 12 and 18 UTC) using the Global Data Assimilation System (GDAS) with a horizontal resolution of 1° × 1°, as the GDAS with 0.5° resolution did not account for vertical motion (Su et al., 2015). The spatial distribution of the number of endpoints for a backward trajectory from four measurement sites revealed the large spatial coverage of the footprint over East Asia

https://doi.org/10.5194/acp-2019-685
Preprint. Discussion started: 2 September 2019


Atmospheric Chemistry and Physics Discussions

(Figure S1). These four sites could be representative for monitoring outflow from China and Korea because of the dominance of wintertime monsoon. Moreover, the footprint of the Noto site could cover the middle part of Japan, such as the Kanto, Chubu, and Kansai regions. To exclude cases with wet deposition influence, the accumulated precipitation along with trajectory (APT) was calculated over the past 72 hours (Kanaya et al., 2016; Oshima et al., 2012), and we only used cases with APT = 0.

As aforementioned, BC and CO are commonly emitted from incomplete fuel combustion, and the ΔBC/ΔCO ratio is used to evaluate the bottom-up emission inventory as a representative indicator preserving the emission ratio when wet removal is not influential (Kanaya et al., 2016). ΔCO was calculated by subtracting the baseline level (determined as a 14-day moving 5th percentile) from the observed CO mixing ratio. On the other hand, ΔBC is the BC concentration as is because the baseline concentration of BC was assumed to be zero. It should be noted that we used the CO concentration when it was higher than the moving 25th percentile of CO, in order to only employ data with meaningful enhancement.

To determine the dominant emission region of each sample, we calculated the residence time over the six regions (East China, North China, Northeast China, North Korea, South Korea, and Japan) using each backward trajectory during the past 72 hours. Hourly endpoints with altitudes less than 2.5 km were counted (Kanaya et al., 2016). Based on the fraction of the total 73 hours, the highest fraction of the region was classified as the dominant emission region when the fraction of frequency was higher than 5% to secure statistics (S1; Figure S2). In addition, we checked (1) the dry deposition effect during traveling time and (2) the influence of other regions on ΔBC/ΔCO depending on the residence time. As a result, there was no significant dry deposition effect (S2; Figure S3) and interrupted by other regions (S3; Figure S4), implying that the BC/CO ratio was preserved regardless of residence time over other regions when the threshold (N > 5) of each bin (20% interval) was satisfied.

3 Results and discussion

3.1 Seasonal variation in BC and CO

The BC, CO, and ΔCO concentrations are summarized in Table 2. The mean BC and ΔCO concentrations were highest in Baengnyeong, followed by Fukuoka, Gosan, and Noto,

https://doi.org/10.5194/acp-2019-685
Preprint. Discussion started: 2 September 2019

Atmospheric Chemistry and Physics Discussions

according to the distance from the main BC and CO emission sources, China. Although the levels at Baengnyeong and Gosan were high, they maintained regional representativeness, as the BC concentration levels were lower than those at urban sites such as Daejon (1.78 μg m^{-3}), Seoul (1.52 μg m^{-3}), and Gwangju (1.13 μg m^{-3}) in Korea (Yu et al., 2018). Despite the suburban location of Fukuoka, the BC and ΔCO concentrations were even lower than those of Baengnyeong, indicating that the measurement site could not be seriously influenced by local sources. In the case of Noto, the BC concentration was lowest among the sites as 0.24 μg m^{-3}. The concentration level was lower than the annual average of 0.36 μg m^{-3} at Fukue (Kanaya et al., 2016) and 0.29 μg m^{-3} at Cape Hedo (Verma et al., 2011), regarded as background monitoring sites in Japan. The seasonal variation in BC concentration at all sites showed similar patterns of being low in summer due to rainout followed by precipitation and increasing from fall due to house heating and/or crop biomass burning along with transition to westerly winds.

Figure 2 shows the time series of BC, CO, ΔBC/ΔCO ratio and APTs at the Noto site. Regardless of precipitation during the measurement periods, the correlation coefficient (R) between BC and CO was 0.70 within the significance level ($p < 0.01$), indicating that BC and CO were emitted from similar sources. Additionally, the R between ΔBC/ΔCO and APT showed a slightly negative relationship as -0.24 within the significance level ($p < 0.01$), suggesting that the wet removal process removed BC, which resulted in a low ΔBC/ΔCO ratio. However, compared to Noto, the other sites showed a weak negative relationship within the significance level ($p < 0.01$) because the amount of APT for the other three sites was lower than that for Noto, which led to less distinctive wet removal effects (Table 2).

3.2 Regional variation in the ΔBC/ΔCO ratio

Figure 3 shows a comparison of the ΔBC/ΔCO ratio between REAS emission inventories and measured values at four sites. The solid symbols with error bars satisfy the fraction of frequency (> 5% in Figure S2) and the number of data for each bin ($N > 5$ in Figure S4). The open symbols with a dashed error bar were excluded from the analysis because they did not satisfy the criteria. It should be noted that the total number of data for dominant emission regions in this study were 2.7 times higher than Kanaya et al. (2016) indicating the significant improvement in the representativeness of regional variation. Due to the large spatial variation

https://doi.org/10.5194/acp-2019-685
Preprint. Discussion started: 2 September 2019


Atmospheric Chemistry and Physics Discussions

in BC and CO in the REAS emission inventory depending on the dominant emission regions, the coefficient of variation (CV; standard deviation divided by the mean) of the BC/CO ratio from the REAS emission inventory (0.65, over the six regions) was much higher than those from the measurements (0.09 – 0.13) at each site. The CV from the REAS emission inventory was still as high as 0.27 when the highest (South Korea) and the lowest ratios (North Korea) were excluded. Moreover, the BC/CO ratio from the REAS emission inventory was slightly higher than the measured ratios except for North Korea, indicating that the REAS BC/CO ratio did not represent the real value. The difference in the ratio between the REAS and the measurements will be discussed further in section 3.3.

The ΔBC/ΔCO ratio in North China showed the lowest average value as 6.2 ± 0.5 ng m^{-3} ppb^{-1} among China, followed by East China (averaged 6.8 ± 0.3 ng m^{-3} ppb^{-1}) and Northeast China (averaged 7.9 ± 0.7 ng m^{-3} ppb^{-1}). The ratio for the two or three regions in China showed significant differences at all sites when Welch's t-test or the ANOVA test was applied ($p < 0.05$), except for Baengnyeong. The lower ΔBC/ΔCO ratio in North China than in East China is also reported as 5.3 ± 2.1 and 6.4 ± 2.2 ng m^{-3} ppb^{-1} in Fukue, 7.0 ± 3.3 and 7.5 ± 4.6 ng m^{-3} ppb^{-1} in Cape Hedo, and 6.5 ± 0.4 and 8.8 ± 0.9 ng m^{-3} ppb^{-1} in Mt. Huang, respectively (Kanaya et al., 2016; Pan et al., 2011; Verma et al., 2011). In case of Northeast China, the variation in the ratio over the measurement sites (0.09 of CV) was higher than that over other Chinese regions (0.07 and 0.04 of CV in East China and North China, respectively). The reason why a higher CV was observed even in the same emission source regions is that the pathway of backward trajectories was different depending on the measurement site (Figure S5); the backward trajectory of Noto passed over the eastern region (Heilongjiang), whereas that of Baengnyeong passed over the western region of Northeast China (Liaoning). The information of Northeast China emission obtained from measurements at Gosan might have been more strongly affected by emissions from South Korea than that at Baengnyeong (S4).

The mean ΔBC/ΔCO ratios of North Korea and South Korea were similar as 7.3 and 7.8 ± 1.2 ng m^{-3} ppb^{-1}, respectively. Verma et al. (2011) reported a lower ratio for the Korean peninsula (both South and North Korea) as 5.7 ± 2.0 ng m^{-3} ppb^{-1}. It should be noted that the ΔBC/ΔCO ratios for South Korea estimated from observations at Korean and Japanese sites were significantly different as 8.9 ± 5.3 ng m^{-3} ppb^{-1} and 6.7 ± 3.8 ng m^{-3} ppb^{-1}, respectively ($p \leq 0.01$). These differences were also consistent with previous studies that reported ratios as

https://doi.org/10.5194/acp-2019-685
Preprint. Discussion started: 2 September 2019

Atmospheric Chemistry and Physics Discussions

8.5 ng m^{-3} ppb^{-1} at Gosan (Sahu et al., 2009) and 6.7 ± 3.7 ng m^{-3} ppb^{-1} at Fukue (Kanaya et al., 2016). This different ratio could also be caused by the different influences of the emission source regions, similar to Northeast China. Baengnyeong and Gosan were mainly influenced by the southwestern region of Korea, including the Seoul Metropolitan Area (SMA), whereas the Fukuoka and Noto sites were mainly influenced by the southeastern region of Korea (Figure S6), suggesting the large spatial variation in BC/CO over the Korean peninsula. In case of Japan, the mean ΔBC/ΔCO ratio was 6.8 ± 0.2 ng m^{-3} ppb^{-1}, which was higher than or similar to reported values as 5.9 ± 3.4 ng m^{-3} ppb^{-1} at Fukue, 5.7 ± 0.9 ng m^{-3} ppb^{-1} at Tokyo and 6.3 ± 0.5 ng m^{-3} ppb^{-1} at Nagoya (Kondo et al., 2006; Kanaya et al., 2016). Moreover, there were no significant differences in the ΔBC/ΔCO ratio between Noto and Fukuoka, although the trajectories passed the different regions of Japan (Figure S7), suggesting that the spatial variation in the ΔBC/ΔCO ratio for Japan was smaller than that for South Korea. The higher ΔBC/ΔCO ratio of South Korea could be explained by the higher ratio of diesel to gasoline vehicles in Korea (0.88) than in Japan (0.09) in 2015 (MLIT 2019; MOLIT 2019) because the BC/CO ratio from diesel vehicles is higher than that from gasoline vehicles due to the different carbon atoms content (Zhou et al., 2009; Guo et al., 2017).

3.3 Comparison between the REAS v2.1 and the measured ΔBC/ΔCO ratio

In this section, we investigated the difference in ΔBC/ΔCO between the measured value and the REAS v2.1 emission inventory. We adopted the mean fractional bias (MFB, ranging from -2 to 2) defined by

$$\mathrm{MFB} = \frac{2}{N}\sum_{i=1}^{i=N}\frac{R_i - M_i}{R_i + M_i} \quad (1)$$

where R_i and M_i denote the REAS emission inventory and the measured ratio corresponding to sample i, respectively.

East China showed the lowest MFB value among Chinese regions as 0.12, and the other two regions had similar MFB values as 0.48 for North China and 0.35 for Northeast China, indicating an overestimation of the REAS emission inventory in China. The BC/CO ratio from the REAS emission inventory showed a higher ratio in North China (10.0 ng m^{-3} ppb^{-1}) than in East China (7.7 ng m^{-3} ppb^{-1}), which is an opposite pattern with the measured ratio.

https://doi.org/10.5194/acp-2019-685
Preprint. Discussion started: 2 September 2019

Atmospheric Chemistry and Physics Discussions

Considering that most trajectories passed Nei Mongol (12.5 ng m^{-3} ppb^{-1}) and Hebei (6.6 ng m^{-3} ppb^{-1}) in North China with a lower measured ΔBC/ΔCO ratio, the BC/CO ratio in Nei Mongol was likely overestimated. In Northeast China, the higher BC/CO ratio in Heilongjiang (14.0 ng m^{-3} ppb^{-1} in REAS) than in Liaoning (11.3 ng m^{-3} ppb^{-1} in REAS) was consistent with the tendency of the measured ΔBC/ΔCO ratio.

The BC/CO ratios from the REAS emission inventory for South Korea (23.2 ng m^{-3} ppb^{-1}) and North Korea (3.7 ng m^{-3} ppb^{-1}) were highly over- and underestimated, along with large absolute values of MFB as 0.99 (by factor 3.0) and -0.66 (by factor 2.0), respectively. The ΔBC/ΔCO ratio in South Korea was still found to be 9.6 ± 0.5 ng m^{-3} ppb^{-1} when the condition was restricted to less than the 25th percentile of maximum relative humidity during the past 72 hours (less than 67.2%) to ensure choosing cases without wet deposition effects. Kanaya et al. (2016) pointed out that industry and transport sectors could be the source of the large discrepancy between the REAS emission inventory and the measurements. Although the ratio of the industry sector in South Korea (41.4 ng m^{-3} ppb^{-1}) is also much higher (13 times) than that in Japan, BC and CO from industrial emissions in South Korea only accounted for 13.4% and 7.9% of the total, respectively. Here we identify relative importance from road transport sector; the BC/CO ratio from road transportation in South Korea was 26.8 ng m^{-3} ppb^{-1}, which was 3.6 times higher than the ratio in Japan, 7.4 ng m^{-3} ppb^{-1}. Looking more closely into the transportation sector, the BC/CO ratios from diesel vehicles were similar between S. Korea (120 ng m^{-3} ppb^{-1}) and Japan (109 ng m^{-3} ppb^{-1}), although the BC emissions can vary depending on the installation of the diesel particulate filter.

To easily compare the CO emission rates from gasoline vehicles between South Korea and Japan, we roughly estimated the CO emission factor from gasoline vehicles. This hypothetical CO emission factor was calculated by considering actual mean daily mileages (31 and 12 km day^{-1} for South Korea and Japan, respectively), the actual number of gasoline vehicles in 2008 (MLIT 2016, 2019; MOLIT 2019; TS, 2009) and total CO emission rates in the REAS emission inventory; the hypothetical CO emission factor in Japan (15.8 CO g km^{-1}; 2.82 Tg from 40.8 million) was 6.9 times higher than that in Korea (2.3 CO g km^{-1}; 0.22 Tg from 8.3 million). Underestimation of the hypothetical CO emission factor in South Korea was also observed in motorcycles (2.8 CO g km^{-1}; 0.06 Tg from 1.8 million), which was lower than that in Japan (14.7 g km^{-1}; 0.15 Tg from 1.5 million), assuming the same motorcycle mileages in South

https://doi.org/10.5194/acp-2019-685
Preprint. Discussion started: 2 September 2019


Atmospheric Chemistry and Physics Discussions

Korea. Clearly the hypothetical CO emission factor thus derived for Korea is unlikely, pointing to underestimation of the assumed CO emission rate. We can roughly revise the total CO emission rate (2.2 Tg) from gasoline vehicles (1.48 Tg) and motorcycles (0.31 Tg) by applying the hypothetical CO emission factor of Japan. Although the hypothetical CO emission factors had a large uncertainty due to the inaccurate mileage for gasoline vehicles and motorcycles, the revised REAS BC/CO ratio decreased to 7.3 ng m^{-3} ppb^{-1}, closer to that of the observations.

The recently updated Korean emission inventory Clean Air Policy Support System (CAPSS; Lee et al. 2012) based on 2015 also had a high BC/CO ratio as 25.1 ng m^{-3} ppb^{-1} (Table 3), with much lower hypothetical CO emission factors for gasoline vehicles (1.1 g km^{-1}) and motorcycles (1.7 g km^{-1}) with similar mean mileage values (30.4 km day^{-1}; TS, 2015), suggesting that BC and CO emissions still need to be improved. This high BC/CO ratio (35.8 ng m^{-3} ppb^{-1}) was also found in the MIX emission inventory (Li et al., 2017), whereas the BC/CO ratio from the Emissions Database for Global Atmospheric Research (EDGAR version 4.3.2; Crippa et al. 2018) inventory in 2010 was much closer to the measured ratio as 7.68 ng m^{-3} ppb^{-1}. Many researchers have been trying to improve the accuracy of the CO emission rate in South Korea from bottom-up emission inventory (0.90 Tg) and top-down estimation (1.10 Tg) derived from the KORUS-AQ campaign (Table 3). However, discrepancies still existed in not only the $\Delta BC/\Delta CO$ ratio but also the CO emission rate. In particular, the CO emission rate in South Korea showed large variations according to the emission inventory, suggesting that CO emission rates over South Korea should be improved preferentially.

In case of North Korea, the CO emission rate (5.14 Tg) from REAS version 2.1 was considerably higher than that of South Korea by a factor of 7.4 and especially higher than that of Japan, resulting in a low BC/CO ratio as 3.7 ng m^{-3} ppb^{-1}. The domestic and industrial sectors in North Korea showed relatively low BC/CO ratio as 6.79 and 4.45 ng m^{-3} ppb^{-1}, respectively, compared to China (9.5 – 10.5 ng m^{-3} ppb^{-1} for industry and 13.9 – 15.6 ng m^{-3} ppb^{-1} for domestic sector). BC and CO emission rates were under- and/or overestimated, respectively, although the quality of fuel and/or end-of-pipe technology could be different. In addition, when we considered registered vehicles in North Korea (0.26 million) and South Korea (16.8 million), the CO emission from road transportation in North Korea (1.75 Tg) is similar with the roughly revised CO emission in South Korea (1.89 Tg), implying a highly overestimated CO emission rate for the transportation sector (Statics of Korea, 2017). The

https://doi.org/10.5194/acp-2019-685
Preprint. Discussion started: 2 September 2019


Atmospheric Chemistry and Physics Discussions

355 Comprehensive Regional Emissions inventory for Atmospheric Transport Experiment
356 (CREATE; Woo et al., 2014) in 2015 and EDGAR reported a much lower CO emission rate in
357 North Korea (1.41 and 1.55 Tg, respectively). As a result, the BC/CO ratio from EDGAR falls
358 within a reasonable range as 6.85 ng m^{-3} ppb^{-1}, indicating agreement with the measured ratio
359 (7.3 ng m^{-3} ppb^{-1}). Kim and Kim (2019) pointed out that the uncertainty in the CO emission
360 rate in North Korea could result from inaccurate emission factors for biofuel compared to fossil
361 fuels because the REAS emission inventory included several biofuel sources (such as fuel wood,
362 crop residue, and animal waste).

363 The mean ΔBC/ΔCO ratio in Japan showed good consistency between the REAS emission
364 inventory (6.84 ng m^{-3} ppb^{-1}) along with lowest absolute MFB as -0.05, close to 0.09 from
365 Kanaya et al. (2016). The BC and CO emission rates from EDGAR, MIX and ECLIPSE V5a
366 were close to those from the REAS emission inventory, indicating that BC and CO emission
367 rates over Japan were more accurate than those over other regions.

368

369 **3.4 Seasonal variation in the ΔBC/ΔCO ratio**

370 The regional ΔBC/ΔCO ratio in the previous sections might still contain variability because
371 of spatial (the difference in the pathways of trajectories) and/or temporal variation (the
372 difference in monthly emission) even in the same dominant emission region. To explore this
373 finer spatio-temporal variability in the ΔBC/ΔCO ratio, the monthly BC and CO emission rates
374 in each grid (0.25° by 0.25°) in the REAS emission inventory were integrated over the pathway
375 of the backward trajectory satisfying altitudes ≤ 2500m and were compared with the
376 observations. Figure 4 shows the seasonal variation in the recalculated BC/CO ratio from the
377 REAS emission inventory and the measured ΔBC/ΔCO ratio regardless of the measurement
378 sites.

379 The recalculated BC/CO ratios of China and North Korea showed similar seasonal variations,
380 relatively high in winter and low in summer. This result is caused by the seasonal variation in
381 the BC emission rate (CV: 0.11 – 0.17) being higher than that in the CO emission rate (CV:
382 0.07 – 0.14) from REAS in China, and domestic heating is the main factor for seasonality. In
383 contrast, the seasonal pattern in the REAS BC/CO ratios of South Korea and Japan, higher in
384 summer than in spring or winter, can be explained by the term of the CO emission rate (CV:

https://doi.org/10.5194/acp-2019-685
Preprint. Discussion started: 2 September 2019


Atmospheric Chemistry and Physics Discussions

385 0.05 for South Korea and 0.12 for Japan) compared to BC (CV: 0.005 for South Korea and 0.03
386 for Japan), which showed a relatively constant rate all year round.

387 The average absolute MFB of ΔBC/ΔCO between the recalculated REAS and the measured
388 values in all regions was 0.28, and that in spring was the lowest as 0.18, followed by fall (0.33),
389 winter (0.33) and summer (0.60). However, the MFB in summer decreased to 0.30, close to
390 that in fall and winter, when the low ΔBC/ΔCO ratio in North China and Northeast China was
391 excluded due to the small number of data. The MFB in South Korea was too high, ranging from
392 0.64 to 0.93, due to underestimation of the CO emission rate, as discussed in section 3.3. It
393 should be noted that the measured ΔBC/ΔCO ratios in spring were the highest among the
394 seasons for all dominant emission regions except for North Korea; in particular, those in East
395 China, South Korea, and Japan showed significant differences in the ΔBC/ΔCO ratios between
396 spring and winter ($p \leq 0.05$). These higher ΔBC/ΔCO ratios in spring than in winter were also
397 observed at Hedo, Okinawa (Verma et al., 2011). This difference might be caused by the
398 seasonality of BC emissions from the domestic sector between spring and winter, which was
399 overwhelmed by the seasonality of CO emissions. The annual consumption of coal (high
400 BC/CO ratios) for household was slightly decreased from 100.4 to 93.5 million tons, whereas
401 that of natural gas (non-emitted BC) showed a significant increase from 7.9 to 36 billion m^3 as
402 a factor of 3.6 times from 2005 to 2015 (National Bureau of Statistics of China, 2017). This
403 fuel transition for the domestic sector could have caused a decreased ΔBC/ΔCO ratio in winter
404 by constant BC emission rate along with increasing CO emission rate.

405 Although the ΔBC/ΔCO in Japan showed good agreement with the regional REAS BC/CO
406 ratio, the mean absolute MFB was 0.29, which was not low, as we expected. In the REAS
407 emission inventory, the CO emission rates in South Korea and Japan mainly varied due to the
408 domestic sector and road transportation, respectively, and those rates were maximum in winter
409 and minimum in summer. The reason why the observed ΔBC/ΔCO ratio in both South Korea
410 and Japan showed the highest values in spring and not summer is that the ratio of ΔBC in spring
411 to summer was higher than the ratio of ΔCO, implying that seasonal variations in CO emission
412 rate could not represent the seasonal characteristics.

413

https://doi.org/10.5194/acp-2019-685
Preprint. Discussion started: 2 September 2019

Atmospheric Chemistry and Physics Discussions

3.5 Estimated potential region of over- and underestimation for ΔBC/ΔCO

Investigation of the potential locations for over- and underestimated ΔBC/ΔCO ratios is performed using a potential source contribution function (PSCF). Typically, PSCF has been widely applied to identify the source regions of aerosols on regional scales, as well as to identify the long-range transported pollution to a receptor site (Guo et al., 2015; Kim et al., 2016). Unlike the grid size of the REAS emission inventory, the trajectory endpoints are assigned to the cells of 0.5° × 0.5° geographic coordinates with latitude (*i*) and longitude (*j*), and the number of trajectory segment endpoints within the grid cell is counted. The PSCF at the *ij*th grid cell can be calculated by the following:

$$PSCF_{i,j} = \frac{\sum m_{i,j}}{\sum n_{i,j}}$$

where $n_{i,j}$ is the total number of trajectory endpoints over the *ij*th grid cell and $m_{i,j}$ is the number of these endpoints that correspond to values higher or lower than a certain criteria over a certain grid cell. We applied MFB values higher than 0.5 and lower than -0.5 for over- and underestimated criteria, respectively. If the total number of trajectory segment endpoints in a particular cell ($\sum n_{i,j}$) is small, the PSCF value may be biased toward overestimation, especially when the value of $\sum m_{i,j}$ is higher at the receptor site. To reduce the effect of abnormal and large $PSCF_{ij}$ values with low $\sum n_{i,j}$, a weight function (Guo et al., 2015) was applied with the power law of the total number of trajectories ($N_{APT=0}$ for each site in Table 2).

For overestimated cases (MFB ≥ 0.5; Figure 5), South Korea was clearly identified as a region with a higher PSCF value regardless of the measurement sites. In particular, the western region of South Korea, including the SMA and the southwestern region, showed the highest PSCF. High PSCF values in Baengnyeong were observed in the SMA region (17.2 ng m^{-3} ppb^{-1} from REAS) with 0.60, whereas those in Gosan were located in the southwestern region of Korea (30.7 ng m^{-3} ppb^{-1} from REAS) with 0.65, suggesting that the southwestern region of Korea is more overestimated than the SMA region. Although the measured ΔBC/ΔCO ratio was similar at Fukuoka and Noto, the overestimated region for Fukuoka was more emphasized in SMA with a higher PSCF value (0.61) than that for Noto, which indicated the southeastern region (27.0 ng m^{-3} ppb^{-1} from REAS) with relatively low PSCF (0.42). In China, Liaoning

https://doi.org/10.5194/acp-2019-685
Preprint. Discussion started: 2 September 2019


Atmospheric Chemistry and Physics Discussions

(10.8 ng m^{-3} ppb^{-1} from REAS) in the Northeast China revealed the highest PSCF (0.43), followed by Tianjin (7.0 ng m^{-3} ppb^{-1} from REAS) in the North China at Baengnyeong, along with similar results in Gosan. Fukuoka and Noto did not directly point out the overestimation regions in China. Nonetheless, Noto may indicate that Heilongjiang (14.0 ng m^{-3} ppb^{-1}) is related to a large overestimation of the ratio, as deduced from the pathway of airmass toward Northeast China. For Japan, the Kyushu and central region (Kansai, Kanto, and Chubu) showed moderate PSCF values (~0.3), implying relatively good consistency between the REAS and the measured ratio.

On the other hand, a PSCF value higher than 0.2 for the underestimated case (MFB ≤ -0.5, Figure 6) was observed only at the Baengnyeong site for North Korea. The most underestimated regions were identified as the western regions of North Korea, such as Pyongyang (4.72 ng m^{-3} ppb^{-1} from REAS) and nearby. Those regions showed the highest CO emission rates (Figure 1), especially from the industrial sector, suggesting that the accuracy of the CO emission rate from not only road transportation but also the industrial sector should be improved. The result from PSCF analysis provided useful information of the potentially over- and underestimated BC/CO ratio region where the BC and CO emission rates should be preferentially updated.

4 Conclusions

To verify the REAS bottom-up emission inventory, the ΔBC/ΔCO ratios were diagnosed from long-term, best-effort observations at four sites in East Asia, including two sites in Korea (Baengnyeong and Gosan) and two sites in Japan (Fukuoka and Noto). Based on the backward trajectories during the past 72 hours, dominant emission regions were assigned to six study domains divided by country and/or administrative district, including three Chinese regions (East, North, and Northeast), two Korean peninsula regions (South and North Korea), and Japan. To choose cases without wet deposition effects, the ΔBC/ΔCO ratio was considered only when the accumulated precipitation along a backward trajectory (APT) for three days was equal to zero.

The regional ΔBC/ΔCO ratios were overestimated in the REAS emission inventory from East, North and Northeast China. The REAS BC/CO ratio of South Korea was 3.0 times higher

https://doi.org/10.5194/acp-2019-685
Preprint. Discussion started: 2 September 2019


Atmospheric Chemistry and Physics Discussions

than the measured ΔBC/ΔCO ratios, whereas Japan showed good consistency between two ratios. The plausible reason was that the CO emissions rate from gasoline vehicles and motorcycles in South Korea were highly underestimated when considering hypothetical CO emission factors compared to those in Japan. However, North Korea revealed a highly underestimated region by a factor of 2.0 due to unrealistically overestimated CO emissions from vehicles, although it is hard to directly compare these emissions with those in other countries due to the possibility of differences in fuel usage and combustion technology. The seasonal variation in the ΔBC/ΔCO ratio revealed different tendencies. The BC/CO ratio from REAS peaked in winter (China and North Korea) or in summer (South Korea and Japan). In contrast, the measured ratio was the highest in spring, implying that the REAS emission inventory did not reflect the major seasonality driver. From the PSCF analysis, the potentially over- and underestimated regions were emphasized in the SMA and southwestern regions of South Korea and Pyongyang of North Korea, respectively. Except for those highlighted regions in the Korean peninsula, a moderate PSCF value for overestimation was also observed at Tianjin (East), Liaoning and Heilongjiang (Northeast) in China and Kyushu and the central region in Japan.

This study provided the overall mean BC/CO ratio with uncertainty for each dominant emission region by taking into consideration the full range of the ΔBC/ΔCO ratio based on spatial (four sites) and temporal variations (four seasons) (Table 3). The BC emissions over East Asia can be estimated by multiplying the observed ΔBC/ΔCO ratio by reliable estimates of the CO emission rate. The discrepancy in the BC/CO ratio is largely contributed from inaccurate CO emission rate in the emission inventory, in addition to the BC emission factors. Therefore, to enhance the accuracy of the BC emission rate over East Asia, a comprehensive and in-depth investigation of CO emissions should be performed to accurately assess the CO emissions rate by considering not only the annual total but also the monthly basis, particularly in the Korean peninsula.

Author contributions

YC and YK designed the study and prepared the manuscript with contributions from all co-authors. SMP, HK and DHJ are responsible for measurements at Baengnyeong. AM and YS

https://doi.org/10.5194/acp-2019-685
Preprint. Discussion started: 2 September 2019

conducted measurements at Noto and IU provided the data at Fukuoka. SWK and ML contributed to ground observation and quality control at Gosan. XP contributed the data analysis. All co-authors provided professional comments to improve the manuscript.

Acknowledgments

This research was supported by the Environment Research and Technology Development Fund (2-1803) of the Ministry of the Environment, Japan. The authors thank NOAA ARL for providing the HYSPLIT backward trajectories.

References

Bond, T. C., Anderson, T. L., and Campbell, D.: Calibration and Intercomparison of Filter-Based Measurements of Visible Light Absorption by Aerosols, Aerosol Sci. Technol., 30, 582-600, 10.1080/027868299304435, 1999.

Bond, T. C., Doherty, S. J., Fahey, D., Forster, P., Berntsen, T., DeAngelo, B., Flanner, M., Ghan, S., Kärcher, B., and Koch, D.: Bounding the role of black carbon in the climate system: A scientific assessment, J. Geophys. Res. Atmos., 118, 5380-5552, 2013.

Cho, C., Kim, S.-W., Lee, M., Lim, S., Fang, W., Gustafsson, Ö., Andersson, A., Park, R. J., and Sheridan, P. J.: Observation-based estimates of the mass absorption cross-section of black and brown carbon and their contribution to aerosol light absorption in East Asia, Atmos. Environ., 212, 65-74, https://doi.org/10.1016/j.atmosenv.2019.05.024, 2019.

Crippa, M., Guizzardi, D., Muntean, M., Schaaf, E., Dentener, F., van Aardenne, J. A., Monni, S., Doering, U., Olivier, J. G. J., Pagliari, V., and Janssens-Maenhout, G.: Gridded emissions of air pollutants for the period 1970–2012 within EDGAR v4.3.2, Earth Syst. Sci. Data, 10, 1987-2013, 10.5194/essd-10-1987-2018, 2018.

Draxler, R,. Stunder, B., Rolph, G., Stein, A., Taylor, A.: HYSPLIT4 user's guide, version 4, http://www.arl.noaa.gov/documents/reports/hysplit_user_guide.pdf, last access: 27 Jun 2019, 2018.

Geng, F., Hua, J., Mu, Z., Peng, L., Xu, X., Chen, R., and Kan, H.: Differentiating the associations of black carbon and fine particle with daily mortality in a Chinese city, Environmental Research, 120, 27-32, https://doi.org/10.1016/j.envres.2012.08.007, 2013.

Guo, Q., Hu, M., Guo, S., Wu, Z., Hu, W., Peng, J., Hu, W., Wu, Y., Yuan, B., Zhang, Q., and Song, Y.: The identification of source regions of black carbon at a receptor site off the eastern coast of China, Atmos. Environ., 100, 78-84, http://dx.doi.org/10.1016/j.atmosenv.2014.10.053, 2015.

Guo, Q., Hu, M., Guo, S., Wu, Z., Peng, J., and Wu, Y.: The variability in the relationship between black carbon and carbon monoxide over the eastern coast of China: BC aging

https://doi.org/10.5194/acp-2019-685
Preprint. Discussion started: 2 September 2019

Atmospheric Chemistry and Physics Discussions

during transport, Atmos. Chem. Phys., 17, 10395-10403, 10.5194/acp-17-10395-2017, 2017.

Han, S., Kondo, Y., Oshima, N., Takegawa, N., Miyazaki, Y., Hu, M., Lin, P., Deng, Z., Zhao, Y., Sugimoto, N., and Wu, Y.: Temporal variations of elemental carbon in Beijing, J. Geophys. Res. Atmos., 114, doi:10.1029/2009JD012027, 2009.

Huebert, B. J., Bates, T., Russell, P. B., Shi, G., Kim, Y. J., Kawamura, K., Carmichael, G., and Nakajima, T.: An overview of ACE-Asia: Strategies for quantifying the relationships between Asian aerosols and their climatic impacts, J. Geophys. Res. Atmos., 108, doi:10.1029/2003JD003550, 2003.

Itahashi, S., Uno, I., Osada, K., Kamiguchi, Y., Yamamoto, S., Tamura, K., Wang, Z., Kurosaki, Y., and Kanaya, Y.: Nitrate transboundary heavy pollution over East Asia in winter, Atmos. Chem. Phys., 17, 3823-3843, 10.5194/acp-17-3823-2017, 2017.

Jacobson, M. Z.: Strong radiative heating due to the mixing state of black carbon in atmospheric aerosols, Nature, 409, 695, 10.1038/35055518.

Janssen, N., A. H., Hoek, G., Simic-Lawson, M., Fischer, P., van Bree, L., ten Brink, H., Keuken, M., Atkinson Richard, W., Anderson, H. R., Brunekreef, B., and Cassee Flemming, R.: Black Carbon as an Additional Indicator of the Adverse Health Effects of Airborne Particles Compared with PM10 and PM2.5, Environ. Health Perspect., 119, 1691-1699, 10.1289/ehp.1003369, 2011.

Janssen, N. A., Gerlofs-Nijland, M. E., Lanki, T., Salonen, R. O., Cassee, F., Hoek, G., Fischer, P., Brunekreef, B., and Krzyzanowski, M.: Health effects of black carbon, WHO Regional Office for Europe Copenhagen, 2012.

Kanaya, Y., Komazaki, Y., Pochanart, P., Liu, Y., Akimoto, H., Gao, J., Wang, T., and Wang, Z.: Mass concentrations of black carbon measured by four instruments in the middle of Central East China in June 2006, Atmos. Chem. Phys., 8, 7637-7649, 10.5194/acp-8-7637-2008, 2008.

Kanaya, Y., Taketani, F., Komazaki, Y., Liu, X., Kondo, Y., Sahu, L. K., Irie, H., and Takashima, H.: Comparison of Black Carbon Mass Concentrations Observed by Multi-Angle Absorption Photometer (MAAP) and Continuous Soot-Monitoring System (COSMOS) on Fukue Island and in Tokyo, Japan, Aerosol Sci. Technol., 47, 1-10, 10.1080/02786826.2012.716551, 2013.

Kanaya, Y., Pan, X., Miyakawa, T., Komazaki, Y., Taketani, F., Uno, I., and Kondo, Y.: Long-term observations of black carbon mass concentrations at Fukue Island, western Japan, during 2009–2015: constraining wet removal rates and emission strengths from East Asia, Atmos. Chem. Phys., 16, 10689-10705, 10.5194/acp-16-10689-2016, 2016.

Kim, B. M., Seo, J., Kim, J. Y., Lee, J. Y., and Kim, Y.: Transported vs. local contributions from secondary and biomass burning sources to PM2.5, Atmos. Environ., 144, 24-36, https://doi.org/10.1016/j.atmosenv.2016.08.072, 2016.

Kim, I. S., and Kim, Y. P.: Characteristics of Energy Usage and Emissions of Air Pollutants in North Korea, J. Korean Soc. Atmos. Environ., 35, 125-137, 2019.

Kondo, Y., Komazaki, Y., Miyazaki, Y., Moteki, N., Takegawa, N., Kodama, D., Deguchi, S.,

https://doi.org/10.5194/acp-2019-685
Preprint. Discussion started: 2 September 2019

Atmospheric Chemistry and Physics Discussions

Nogami, M., Fukuda, M., Miyakawa, T., Morino, Y., Koike, M., Sakurai, H., and Ehara, K.: Temporal variations of elemental carbon in Tokyo, J. Geophys. Res. Atmos., 111, doi:10.1029/2005JD006257, 2006.

Kondo, Y.: Effects of black carbon on climate: Advances in measurement and modeling, Monogr. Environ. Earth Planets, 3, 1-85, 2015.

Kurokawa, J., Ohara, T., Morikawa, T., Hanayama, S., Janssens-Maenhout, G., Fukui, T., Kawashima, K., and Akimoto, H.: Emissions of air pollutants and greenhouse gases over Asian regions during 2000–2008: Regional Emission inventory in ASia (REAS) version 2, Atmos. Chem. Phys., 13, 11019-11058, 10.5194/acp-13-11019-2013, 2013.

Li, M., Zhang, Q., Kurokawa, J. I., Woo, J. H., He, K., Lu, Z., Ohara, T., Song, Y., Streets, D. G., Carmichael, G. R., Cheng, Y., Hong, C., Huo, H., Jiang, X., Kang, S., Liu, F., Su, H., and Zheng, B.: MIX: a mosaic Asian anthropogenic emission inventory under the international collaboration framework of the MICS-Asia and HTAP, Atmos. Chem. Phys., 17, 935-963, 10.5194/acp-17-935-2017, 2017.

Lim, S., Lee, M., Lee, G., Kim, S., Yoon, S., and Kang, K.: Ionic and carbonaceous compositions of PM10, PM2.5 and PM1.0 at Gosan ABC Superstation and their ratios as source signature, Atmos. Chem. Phys., 12, 2007-2024, 10.5194/acp-12-2007-2012, 2012.

Loomis, D., Grosse, Y., Lauby-Secretan, B., Ghissassi, F. E., Bouvard, V., Benbrahim-Tallaa, L., Guha, N., Baan, R., Mattock, H., and Straif, K.: The carcinogenicity of outdoor air pollution, Lancet Oncol., 14, 1262-1263, https://doi.org/10.1016/S1470-2045(13)70487-X, 2013.

Miyakawa, T., Oshima, N., Taketani, F., Komazaki, Y., Yoshino, A., Takami, A., Kondo, Y., and Kanaya, Y.: Alteration of the size distributions and mixing states of black carbon through transport in the boundary layer in east Asia, Atmos. Chem. Phys., 17, 5851-5864, 10.5194/acp-17-5851-2017, 2017.

Miyazaki, K., Sekiya, T., Fu, D., Bowman, K. W., Kulawik, S. S., Sudo, K., Walker, T., Kanaya, Y., Takigawa, M., Ogochi, K., Eskes, H., Boersma, K. F., Thompson, A. M., Gaubert, B., Barre, J., and Emmons, L. K.: Balance of Emission and Dynamical Controls on Ozone During the Korea-United States Air Quality Campaign From Multiconstituent Satellite Data Assimilation, J. Geophys. Res. Atmos., 124, 387-413, doi:10.1029/2018JD028912, 2019.

MLIT (Ministry of Land, Infrastructure, Transport and Tourism): Annual report of Automobile transportation statistics in 2015, https://www.e-stat.go.jp/stat-search/file-download?statInfId=000031752810&fileKind=2, last access: 25 Jan 2019, 2016 (in Japanese).

MLIT: Traffic statistics book, http://www.mlit.go.jp/statistics/kotsusiryo.html, last access: 27 June 2019 (in Japanese).

MOLIT (Ministry of Land, Infrastructure and Transport): Total Registered Moter Vehicles, http://stat.molit.go.kr/portal/cate/statFileView.do?hRsId=58&hFormId=5..., last access: 8 Feb 2019 (in Korean).

Myhre, G., Shindell, D., Bréon, F.-M., Collins, W., Fuglestvedt, J., Huang, J., Koch, D., Lamarque, J.-F., Lee, D., and Mendoza, B., Nakajima, T., Robock, A., Stephens, G.,

https://doi.org/10.5194/acp-2019-685
Preprint. Discussion started: 2 September 2019

Atmospheric Chemistry and Physics Discussions

Takemura, T., and Zhang, H.: Anthropogenic and Natural Radiative Forcing. In: Climate Change 2013: The Physical Science Basis. Contribution of Working Group I to the Fifth Assessment Report of the Intergovernmental Panel on Climate Change, Cambridge University Press, Cambridge, United Kingdom and New York, NY, USA, 2013.

Nakajima, T., Yoon, S.-C., Ramanathan, V., Shi, G.-Y., Takemura, T., Higurashi, A., Takamura, T., Aoki, K., Sohn, B.-J., Kim, S.-W., Tsuruta, H., Sugimoto, N., Shimizu, A., Tanimoto, H., Sawa, Y., Lin, N.-H., Lee, C.-T., Goto, D., and Schutgens, N.: Overview of the Atmospheric Brown Cloud East Asian Regional Experiment 2005 and a study of the aerosol direct radiative forcing in east Asia, J. Geophys. Res. Atmos., 112, doi:10.1029/2007JD009009, 2007.

National Bureau of Statistics of China: China Statistical Yearbook 2017, China Statistics Press, Beijing, ISBN-13: 978-7503782534, 2017.

NIOSH: Method 5040 issue 1: elemental carbon (diesel exhaust), 4th ed., Cincinnati, OH, 1996.

Ogren, J. A., Wendell, J., Andrews, E., and Sheridan, P. J.: Continuous light absorption photometer for long-term studies, Atmos. Meas. Tech., 10, 4805-4818, https://doi.org/10.5194/amt-10-4805-2017, 2017.

Ohara, T., Akimoto, H., Kurokawa, J., Horii, N., Yamaji, K., Yan, X., and Hayasaka, T.: An Asian emission inventory of anthropogenic emission sources for the period 1980–2020, Atmos. Chem. Phys., 7, 4419-4444, 10.5194/acp-7-4419-2007, 2007.

Oshima, N., Kondo, Y., Moteki, N., Takegawa, N., Koike, M., Kita, K., Matsui, H., Kajino, M., Nakamura, H., Jung, J. S., and Kim, Y. J.: Wet removal of black carbon in Asian outflow: Aerosol Radiative Forcing in East Asia (A-FORCE) aircraft campaign, J. Geophys. Res. Atmos., 117, 10.1029/2011JD016552, 2012.

Pan, X. L., Kanaya, Y., Wang, Z. F., Liu, Y., Pochanart, P., Akimoto, H., Sun, Y. L., Dong, H. B., Li, J., Irie, H., and Takigawa, M.: Correlation of black carbon aerosol and carbon monoxide in the high-altitude environment of Mt. Huang in Eastern China, Atmos. Chem. Phys., 11, 9735-9747, 10.5194/acp-11-9735-2011, 2011.

Pan, X. L., Kanaya, Y., Wang, Z. F., Komazaki, Y., Taketani, F., Akimoto, H., and Pochanart, P.: Variations of carbonaceous aerosols from open crop residue burning with transport and its implication to estimate their lifetimes, Atmos. Environ., 74, 301-310, https://doi.org/10.1016/j.atmosenv.2013.03.048, 2013.

Park, S.-S., Jung, S.-A., Gong, B.-J., Cho, S.-Y., and Lee, S.-J.: Characteristics of PM2.5 Haze Episodes Revealed by Highly Time-Resolved Measurements at an Air Pollution Monitoring Supersite in Korea, Aerosol Air Qual. Res., 13, 957-976, 10.4209/aaqr.2012.07.0184, 2013.

Petzold, A., Schloesser, H., Sheridan, P. J., Arnott, W. P., Ogren, J. A., and Virkkula, A.: Evaluation of Multiangle Absorption Photometry for Measuring Aerosol Light Absorption, Aerosol Sci. Technol., 39, 40-51, 10.1080/027868290901945, 2005.

Ramana, M. V., Ramanathan, V., Feng, Y., Yoon, S. C., Kim, S. W., Carmichael, G. R., and Schauer, J. J.: Warming influenced by the ratio of black carbon to sulphate and the black-carbon source, Nature Geoscience, 3, 542–545, , 2010.

https://doi.org/10.5194/acp-2019-685
Preprint. Discussion started: 2 September 2019

Atmospheric Chemistry and Physics Discussions

Ramanathan, V., and Carmichael, G.: Global and regional climate changes due to black carbon, Nature Geoscience, 1, 221, 10.1038/ngeo156, 2008.

Sahu, L. K., Kondo, Y., Miyazaki, Y., Kuwata, M., Koike, M., Takegawa, N., Tanimoto, H., Matsueda, H., Yoon, S. C., and Kim, Y. J.: Anthropogenic aerosols observed in Asian continental outflow at Jeju Island, Korea, in spring 2005, J. Geophys. Res. Atmos., 114, doi:10.1029/2008JD010306, 2009.

Samset, B. H.: How cleaner air changes the climate, Science, 360, 148-150, 10.1126/science.aat1723, 2018.

Smith, K. R., Jerrett, M., Anderson, H. R., Burnett, R. T., Stone, V., Derwent, R., Atkinson, R. W., Cohen, A., Shonkoff, S. B., Krewski, D., Pope, C. A., Thun, M. J., and Thurston, G.: Public health benefits of strategies to reduce greenhouse-gas emissions: health implications of short-lived greenhouse pollutants, The Lancet, 374, 2091-2103, https://doi.org/10.1016/S0140-6736(09)61716-5, 2009.

Su, L., Yuan, Z., Fung, J. C. H., and Lau, A. K. H.: A comparison of HYSPLIT backward trajectories generated from two GDAS datasets, Sci. Total Environ., 506-507, 527-537, https://doi.org/10.1016/j.scitotenv.2014.11.072, 2015.

Statics of Korea: Major Statistics Indicators of North Korea, Statistics Korea, Korea, 287pp, 2017.

Turpin, B. J., Saxena, P., and Andrews, E.: Measuring and simulating particulate organics in the atmosphere: problems and prospects, Atmos. Environ., 34, 2983-3013, https://doi.org/10.1016/S1352-2310(99)00501-4, 2000.

TS (Korea Transportation Safety Authority): A research on the real condition of driving mileage in 2008, https://www.kotems.or.kr/app/kotems/forward?pageUrl=/kotems/ptl/bbs/KotemsPtlBbsStatsLs&topmenu1=06&topmenu2=03&topmenu3=03, last access: 25 Jun 2019, 2009 (In Korean).

TS: A research on the real condition of actual driving mileage in 2015 (2012-2015), https://www.kotems.or.kr/app/kotems/forward?pageUrl=/kotems/ptl/bbs/KotemsPtlBbsStatsLs&topmenu1=06&topmenu2=03&topmenu3=03, last access: 25 Jun 2019, 2016 (In Korean).

Ueda, S., Nakayama, T., Taketani, F., Adachi, K., Matsuki, A., Iwamoto, Y., Sadanaga, Y., and Matsumi, Y.: Light absorption and morphological properties of soot-containing aerosols observed at an East Asian outflow site, Noto Peninsula, Japan, Atmos. Chem. Phys., 16, 2525-2541, 10.5194/acp-16-2525-2016, 2016.

Uno, I., Osada, K., Yumimoto, K., Wang, Z., Itahashi, S., Pan, X., Hara, Y., Kanaya, Y., Yamamoto, S., and Fairlie, T. D.: Seasonal variation of fine- and coarse-mode nitrates and related aerosols over East Asia: synergetic observations and chemical transport model analysis, Atmos. Chem. Phys., 17, 14181-14197, 10.5194/acp-17-14181-2017, 2017.

Verma, R. L., Kondo, Y., Oshima, N., Matsui, H., Kita, K., Sahu, L. K., Kato, S., Kajii, Y., Takami, A., and Miyakawa, T.: Seasonal variations of the transport of black carbon and carbon monoxide from the Asian continent to the western Pacific in the boundary layer, J. Geophys. Res. Atmos., 116, doi:10.1029/2011JD015830, 2011.

https://doi.org/10.5194/acp-2019-685
Preprint. Discussion started: 2 September 2019

Atmospheric Chemistry and Physics Discussions

Wang, Y., Wang, X., Kondo, Y., Kajino, M., Munger, J. W., and Hao, J.: Black carbon and its correlation with trace gases at a rural site in Beijing: Top-down constraints from ambient measurements on bottom-up emissions, J. Geophys. Res. Atmos., 116, doi:10.1029/2011JD016575, 2011.

Woo, J.-H., Choi, K.-C., Kim, H. K., Baek, B. H., Jang, M., and Eum, J.-H.: Development of an anthropogenic emissions processing system for Asia using SMOKE. Atmos. Environ., 58, 5-13, 2012.

Woo, J.-H., Quan, S., Choi, K.-C., Kook, H., Jin, H., Song, C.-K., Han, J., and Lee, S.: Development of the CREATE inventory in support of integrated modeling of climate and air quality for East Asia, GEIA Conference, Boulder, USA, 2014.

Yu, G. H., Park, S. S., Ghim, Y. S., Shin, H. J., Lim, C. S., Ban, S. J., Yu, J. A., Kang, H. J., Seo, Y. K., Kang, K. S., Jo, M. R., Jung, S. A., Lee, M. H., Hwang, T. K., Kang, B. C., and Kim, H. S.: Difference in Chemical Composition of PM2.5 and Investigation of its Causing Factors between 2013 and 2015 in Air Pollution Intensive Monitoring Stations, J. Korean Soc. Atmos. Environ., 34, 16-37, 2018.

Zhou, X., Gao, J., Wang, T., Wu, W., and Wang, W.: Measurement of black carbon aerosols near two Chinese megacities and the implications for improving emission inventories, Atmos. Environ., 43, 3918-3924, https://doi.org/10.1016/j.atmosenv.2009.04.062, 2009.

Zhu, C., Kanaya, Y., Yoshikawa-Inoue, H., Irino, T., Seki, O., and Tohjima, Y.: Sources of atmospheric black carbon and related carbonaceous components at Rishiri Island, Japan: The roles of Siberian wildfires and of crop residue burning in China, Environ. Pollut., 247, 55-63, https://doi.org/10.1016/j.envpol.2019.01.003, 2019.

https://doi.org/10.5194/acp-2019-685
Preprint. Discussion started: 2 September 2019

Atmospheric Chemistry and Physics Discussions

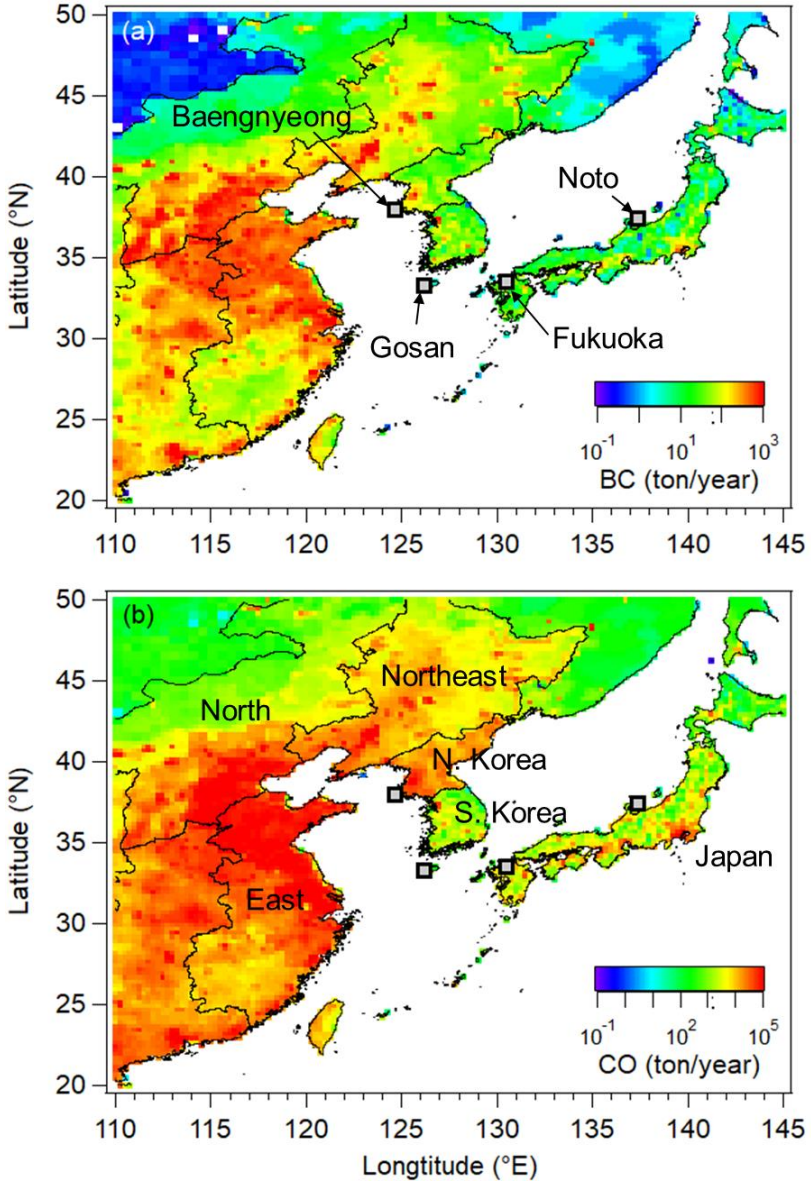

Figure 1. Yearly (a) BC and (b) CO emission rates (ton/year) over East Asia in 2008 from the REAS 2.1 bottom-up emission inventory (Kurokawa et al., 2013). The four measurement sites are shown in (a). (b) shows that the six study domains are divided by country and/or administrative district, including three Chinese regions (East, North, and Northeast), two Korean peninsula regions (South and North Korea), and Japan.

https://doi.org/10.5194/acp-2019-685
Preprint. Discussion started: 2 September 2019

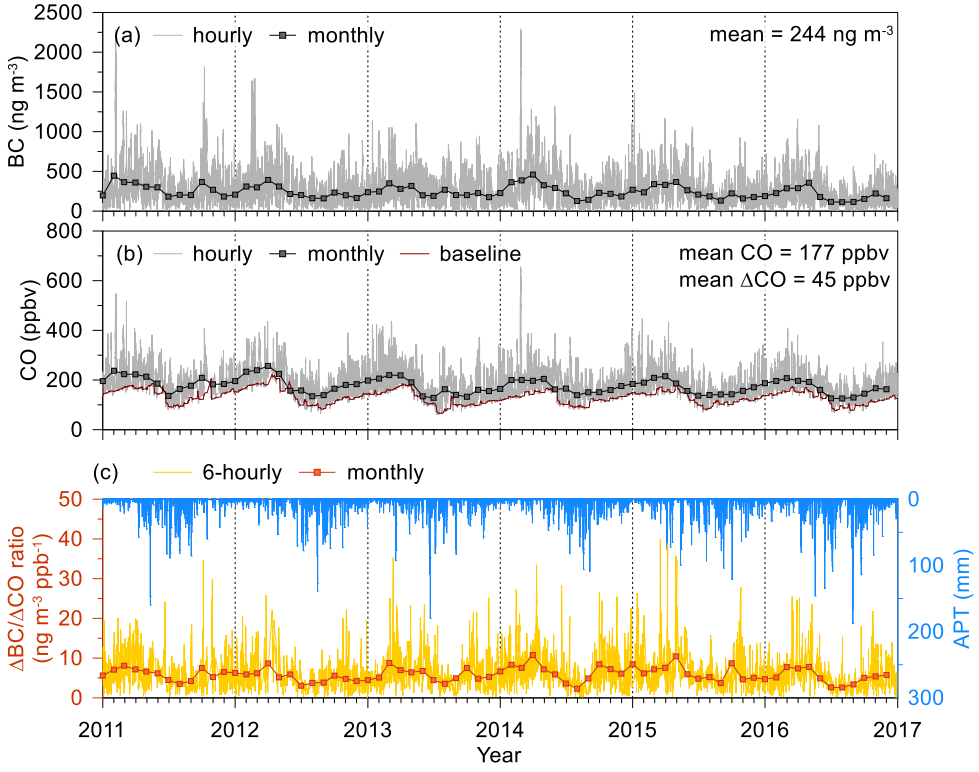

Figure 2. Time series of (a) BC concentration, (b) CO and ΔCO concentrations and (c) ΔBC/ΔCO ratio and accumulated precipitation along with trajectory (APT) during the measurement periods (from 2011 to 2017) in Noto, Japan. The square symbols with solid lines in (a) and (b) indicate hourly and monthly concentrations.

https://doi.org/10.5194/acp-2019-685
Preprint. Discussion started: 2 September 2019

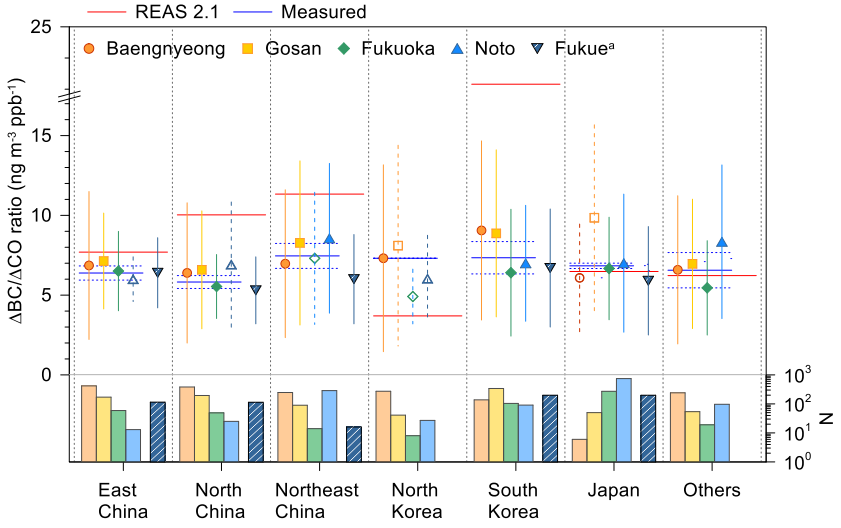

Figure 3. ΔBC/ΔCO ratio in four measurement sites and Fukue from Kanaya et al. (2016) according to the dominant emission regions. The symbols with vertical lines are the mean and standard deviation of the ΔBC/ΔCO ratio. The bar graph on the bottom indicates the number of data in the dominant emission region. Open symbols with dashed vertical lines indicate excluded data because of the low number of data. The solid blue horizontal lines with dashed lines for each region indicate the mean and standard deviation of the measured ΔBC/ΔCO, excluding the areas with limited data. The solid red horizontal lines depict mean BC/CO ratio from the REAS 2.1 emission inventory (Kurokawa et al., 2013).

https://doi.org/10.5194/acp-2019-685
Preprint. Discussion started: 2 September 2019

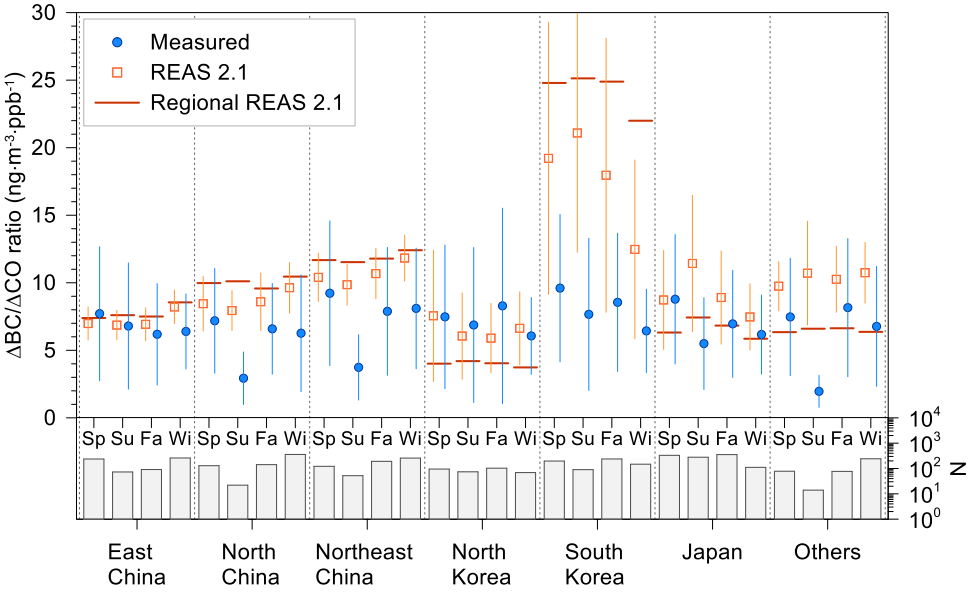

Figure 4. The seasonal ΔBC/ΔCO ratios from four measurement sites depend on the dominant emission region. The horizontal lines for each region indicate the mean value of the ΔBC/ΔCO ratio from the REAS 2.1 emission inventory (Kurokawa et al., 2013). The bar graph on the bottom indicates the number of data in each season and the dominant emission region. The symbols with vertical lines are the mean and standard deviation of the ΔBC/ΔCO ratio. The abbreviation of 'Sp' to 'Wi' indicates spring to winter.

https://doi.org/10.5194/acp-2019-685
Preprint. Discussion started: 2 September 2019

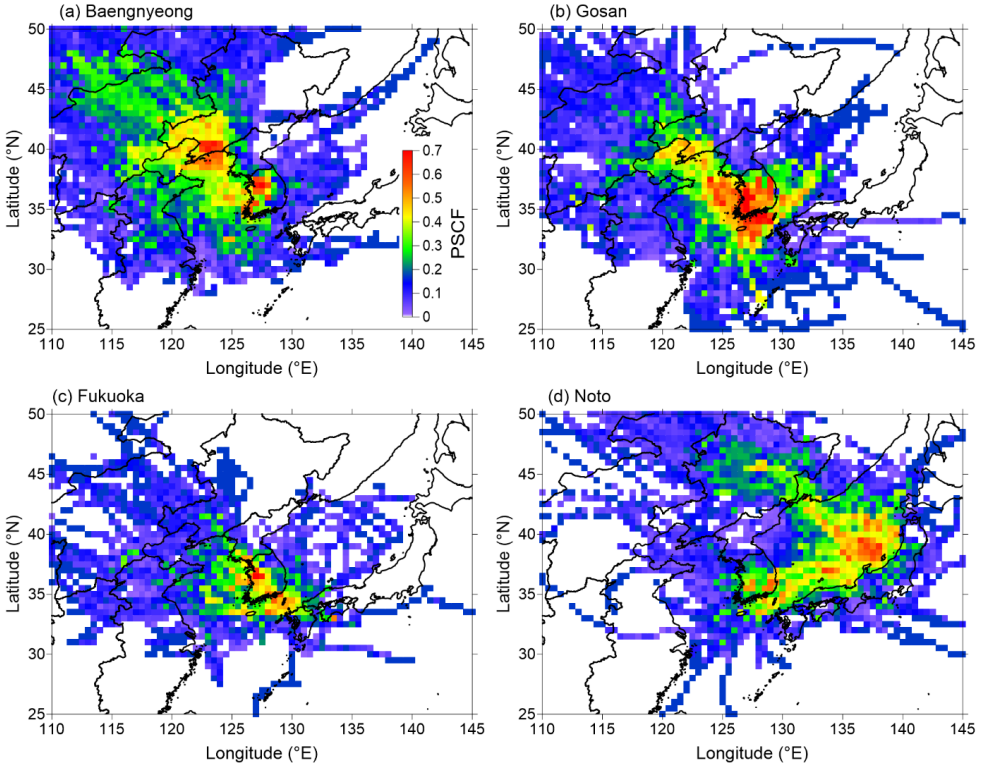

Figure 5. Spatial distribution of the PSCF result for mean fractional bias (MFB) ≥ 0.5 for overestimation cases at the (a) Baengnyeong, (b) Gosan, (c) Fukuoka, and (d) Noto sites. MFB is calculated from $2\times(R_i - M_i)/(R_i + M_i)$, where R_i and M_i denote the mean value for the recalculated REAS BC/CO ratio along with the backward trajectory and the measured BC/CO ratio, respectively.

https://doi.org/10.5194/acp-2019-685
Preprint. Discussion started: 2 September 2019

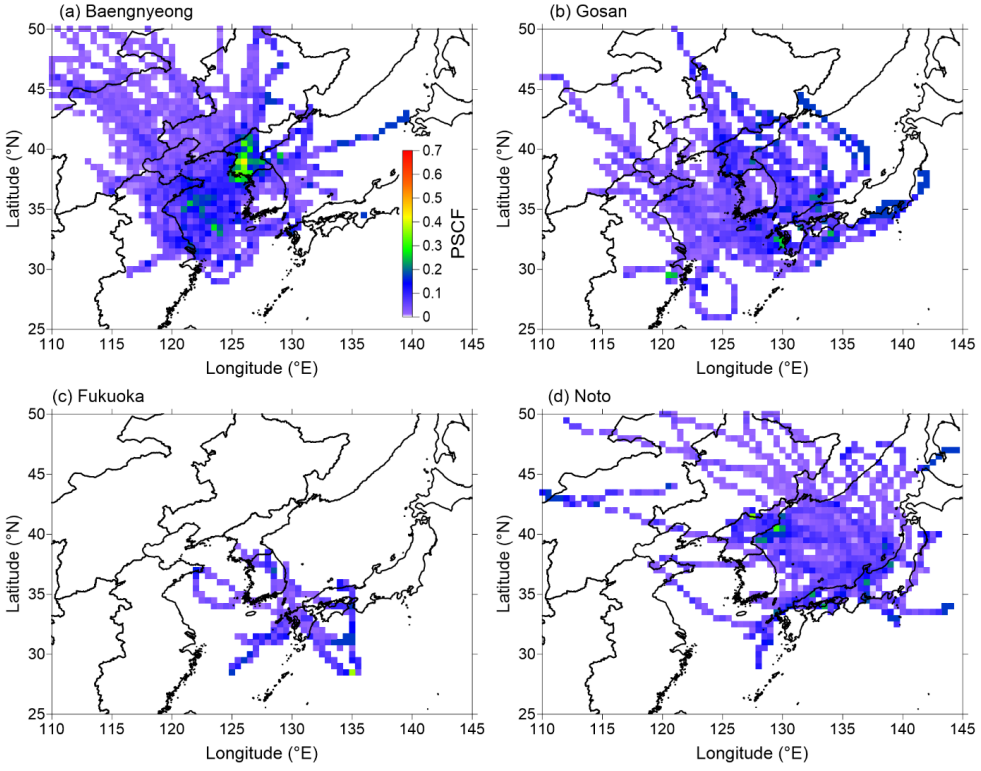

Figure 6. Same as Figure 5 except for mean fractional bias (MFB) ≤ -0.5 for underestimation cases.

Table 1. Description of measurement sites, periods, and instruments.

Sites		Longitude, Latitude	Measurement periods	Instruments
South Korea	Baengnyeong (background)	124.63 °E, 37.97 °N	2010.01.01 – 2016.12.31 (except for 2011 and 2012)	EC: sunset EC/OC CO: Teledyne API 300E
	Gosan (background)	126.17 °E, 33.28 °N	2012.05.01 – 2015.4.30	BC: CLAP[a] CO: Model 48i
Japan	Noto (background)	137.36 °E, 37.45 °N	2011.01.01 – 2016.12.31	BC: MAAP[b] CO: Model 48i
	Fukuoka (suburban area)	130.47 °E, 33.52 °N	2014.09.01 – 2016.03.31	BC: MAAP CO: Model 48i

[a] continuous light absorption photometer, [b] multi-angle absorption photometer

Table 2. Mean and standard deviation of black carbon (BC)[a], carbon monoxide (CO)[b], ΔCO concentrations[b], amount of APT[c] and the number of data for All (N_{all}) and APT=0 ($N_{APT=0}$) cases in each site.

	All	Spring	Summer	Fall	Winter
(a) Baengnyeong					
BC	826.5 ± 304.4	855.8 ± 204.0	561.7 ± 149.7	795.3 ± 300.8	1017.9 ± 347.2
CO	293.1 ± 61.7	317.4 ± 38.6	239.6 ± 41.0	265.4 ± 51.6	340.5 ± 56.1
ΔCO	127.6 ± 46.1	121.2 ± 23.4	100.2 ± 44.3	114.0 ± 40.7	169.0 ± 42.5
APT	3.6 ± 9.1	2.8 ± 6.4	9.1 ± 16.1	2.8 ± 6.5	1.5 ± 3.7
N_{All}	3,828	1,155	764	669	1,240
$N_{APT=0}$	1,793	560	199	339	695
(b) Gosan					
BC	490.2 ± 168.4	659.4 ± 200.4	323.4 ± 92.3	454.6 ± 59.7	542.2 ± 94.8
CO	190.1 ± 49.5	225.9 ± 20.0	128.4 ± 38.5	178.9 ± 29.4	227.1 ± 23.2
ΔCO	81.6 ± 27.2	87.2 ± 15.9	53.8 ± 21.3	77.8 ± 22.2	107.7 ± 18.8
APT	6.4 ± 14.4	4.2 ± 10.3	15.1 ± 23.0	5.2 ± 10.5	1.8 ± 3.6
N_{All}	2,510	395	598	778	739
$N_{APT=0}$	950	185	100	343	322
(c) Fukuoka					
BC	676.5 ± 105.8	665.5 ± 73.4	571.4 ± 43.9	700.0 ± 157.6	715.0 ± 63.3
CO	305.7 ± 43.7	303.6 ± 27.0	251.6 ± 34.7	293.3 ± 36.1	346.5 ± 26.8
ΔCO	124.6 ± 33.3	100.0 ± 22.9	99.6 ± 7.0	125.3 ± 35.4	152.9 ± 24.2
APT	6.4 ± 13.4	7.2 ± 13.7	13.9 ± 20.5	6.0 ± 13.1	3.3 ± 7.5
N_{All}	1,435	286	206	427	516
$N_{APT=0}$	547	114	37	179	217

(d) Noto					
BC	244.6 ± 81.0	339.9 ± 45.3	201.7 ± 54.2	203.1 ± 57.7	233.6 ± 74.6
CO	176.9 ± 31.9	212.1 ± 17.9	148.4 ± 17.1	157.2 ± 20.4	189.9 ± 21.7
ΔCO	45.4 ± 10.7	48.9 ± 7.4	44.8 ± 11.9	42.0 ± 10.9	46.2 ± 11.7
APT	7.9 ± 14.6	7.2 ± 13.9	13.7 ± 20.3	7.9± 13.4	3.2 ± 4.3
N_{All}	6,089	1,482	1,468	1,574	1,565
$N_{APT=0}$	1,290	415	267	353	255

[a] ng m^{-3}; [b] ppbv; [c] mm

https://doi.org/10.5194/acp-2019-685
Preprint. Discussion started: 2 September 2019

Atmospheric Chemistry and Physics Discussions
Open Access
EGU

Table 3. (a) Regional ΔBC/ΔCO (ng m^{-3} ppb^{-1}) ratio and emission rates of (b) BC and (c) CO (in Tg per year) over East Asia from various emission inventories.

	This study[a]	REAS 2.1 (2008)	EDGAR (2010)	MIX (2010)	CAPSS (2015)	ECLIPSE[b] (2015)	KORUS V2[c] (2016)	QA4ECV[d] (2016)
(a) ΔBC/ΔCO								
East China	6.8 ± 0.5	7.70	11.4	11.7		11.3		
North China	6.4 ± 0.5	10.0	12.2	12.9		12.4		
Northeast China	8.2 ± 0.7	11.8	12.0	11.9		12.0		
North Korea	7.2 ± 0.7	3.63	6.85	3.90	-	6.55		
South Korea	7.9 ± 1.2	23.2	7.68	35.8	25.1	4.82	17.8[e]	14.5[e]
Japan	6.8 ± 1.0	6.48	7.27	5.84	-	10.1		
(b) BC								
East China		0.400	0.402[b]	0.400[b]		0.382		
North China		0.331	0.346[b]	0.358[b]		0.355		
Northeast China		0.157	0.160[b]	0.159[b]		0.181		
North Korea		0.015	0.009	0.014	-	0.056	-	
South Korea		0.013	0.032	0.024	0.016	0.027	-	
Japan		0.026	0.031	0.020	-	0.019	-	
(c) CO								
East China		65.0	44.1[b]	42.6[b]		44.4		
North China		41.2	35.5[b]	34.8[b]		33.5		
Northeast China		16.6	16.6[b]	16.8[b]		16.3		
North Korea		5.14	1.55	4.49	-	2.85		
South Korea		0.69	2.56	0.84	0.79	3.32	0.90	1.10
Japan		5.03	3.97	4.28	-	3.23		

[a] With uncertainty (1σ) calculated by regional and seasonal mean values.
[b] Calculated based on administrative division from emission inventory, which did not provide regional emission rate.
[c] Based on the improved CAPSS for 2015 and CREATE v3 in China for 2015 using SMOKE-Asia emission processing at 0.1° resolution (Woo

https://doi.org/10.5194/acp-2019-685
Preprint. Discussion started: 2 September 2019

Atmospheric Chemistry and Physics Discussions

et al., 2012).
[d] From multiconstituent data assimilation. Please find more details in Miyazaki et al. (2019).
[e] Using the BC emission rate from the REAS 2.1 emission inventory